

# Possible Magnetic Chirality in Optically Chiral Magnet [Cr(CN)<sub>6</sub>][Mn(*S*)-pnH(H<sub>2</sub>O)](H<sub>2</sub>O) Probed by Muon Spin Rotation and Relaxation

Kazuki OHISHI<sup>1\*</sup>, Wataru HIGEMOTO<sup>1†</sup>, Akihiro KODA<sup>1</sup>, Shanta R. SAHA<sup>1‡</sup>, Ryosuke KADONO<sup>1,2</sup>, Katsuya INOUE<sup>2,3,4</sup>, Hiroyuki IMAI<sup>3§</sup>, and Hiroyuki HIGASHIKAWA<sup>4</sup>

<sup>1</sup>*Institute of Materials Structure Science, High Energy Accelerator Research Organization (KEK), Tsukuba, Ibaraki 305-0801*

<sup>2</sup>*School of High Energy Accelerator Science, The Graduate University for Advanced Studies, Hayama, Kanagawa 240-0193*

<sup>3</sup>*Institute for Molecular Science, Okazaki National Institutes, Okazaki, Aichi 444-8585*

<sup>4</sup>*Faculty of Science, Hiroshima University, Higashi-Hiroshima, Hiroshima 739-8526*

(Received February 6, 2008)

Local magnetic fields in a molecule-based optically chiral magnet [Cr(CN)<sub>6</sub>][Mn(*S*)-pnH(H<sub>2</sub>O)](H<sub>2</sub>O) (GN-(*S*)) and its enantiomer (GN-(*R*)) are studied by means of muon spin rotation and relaxation ( $\mu$ SR). Detailed analysis of muon precession signals under zero field observed below  $T_C$  supports the average magnetic structure suggested by neutron powder diffraction. Moreover, comparison of  $\mu$ SR spectra between GN-(*S*) and GN-(*R*) suggests that they are a pair of complete optical isomers in terms of both crystallographic and magnetic structure. Possibility of *magnetic* chirality in such a pair is discussed.

KEYWORDS: molecule-based magnets, chiral symmetries, magnetism,  $\mu$ SR

Magneto-optical activity bears a strong phenomenological resemblance to natural (conventional) optical activity in many respects. Both represent a difference in absorption and refraction between left and right circularly polarized light, where the latter occurs in media having crystallographic chirality while the former in media subject to magnetic field parallel to the wave vector of the light. The two effects, however, have completely different origins. Natural optical activity is a result of nonlocal optical response in media that lack mirror symmetry, whereas magneto-optical activity results from the breaking of time-reversal symmetry by a magnetic field. In recent years, optical and magnetic properties of molecule-based magnets have attracted much interests because of their transparency for light and their application. Especially, in the case of a magnet with non-centrosymmetric structure, it is expected that both space-inversion and time-reversal symmetry breaking occurs simultaneously. Moreover, when a magnet is characterized by chiral structure, the magnetic structure of the crystal is expected to induce chiral spin structure. Wagniere and Mejer theoretically predicted that *chiral magnets* (i.e., those in which the magnetic moments take a chiral structure) shows magneto-chiral dichroism (MChD) effect besides the above two effects.<sup>1</sup> (Note that the presence of chirality in the crystallographic structure has no direct relevance to that in the magnetic structure.) While the natural and magneto-optical activities are effective over polarized light, the characteristic of MChD is that it occurs over ordinary light. A small MChD ef-

fect was experimentally observed under a magnetic field in a paramagnetic chiral compound for the first time.<sup>2</sup> However, the observed effect is very small probably because the magnetization is small in this compound. Since MChD effect depends on the bulk magnetization, relatively large effect may be expected in chiral magnets compared with paramagnetic compounds.

Since molecule-based magnets have a flexibility in the design of molecular building blocks and their intermolecular structure including dimensionality, they are open to enormous possibilities to create new magneto-optical materials. As a matter of fact, several optically chiral magnets (which are simply called “chiral magnets” regardless of *magnetic* chirality) have been synthesized as optically active magnetic materials in the recent years.<sup>3–8</sup> One of these new molecule-based materials is a two-dimensional chiral magnet of a green needle-shaped crystals, [Cr(CN)<sub>6</sub>][Mn(*S* or *R*)-pnH(H<sub>2</sub>O)](H<sub>2</sub>O) ((*S* or *R*)-pn: (*S* or *R*)-1,2-diaminopropane, abbreviated as green needles or GN-(*S* or *R*)). (Note that (*S*)-pn and (*R*)-pn are the optical isomers.) The crystal structure of this compound is indexed on the basis of an orthorhombic unit cell with a space group  $P2_12_12_1$ , and lattice constants  $a$ ,  $b$  and  $c$  are estimated to be 7.6280(17) Å, 14.510(3) Å and 14.935(3) Å, respectively. There are two-dimensional planes consisting of Mn and Cr stacking along  $c$  axis. Both zero-field cooled and field cooled magnetization with a low applied field (5 Oe) indicate a magnetic order below 38 K. The saturated magnetization at 5 K is about 2  $\mu_B$ . This value is in good agreement with the theoretical value of antiferromagnetic coupling between Cr<sup>3+</sup> and Mn<sup>2+</sup> ions. These results suggest that GN-(*S*) is a ferrimagnet in which Cr<sup>3+</sup> and Mn<sup>2+</sup> spins are antiparallel on  $a$  axis. The most interesting issue associated with this compound is whether or not it has any chirality in the *magnetic* structure, which is suggested by the enhanced magnetic circular dichroism ef-

\*Present address: Advanced Science Research Center, Japan Atomic Energy Agency. E-mail: ohishi.kazuki@jaea.go.jp

†Present address: Advanced Science Research Center, Japan Atomic Energy Agency.

‡Present address: Department of Physics and Astronomy, McMaster University.

§Present address: Department of Chemistry, Faculty of Science, Hokkaido University.

fect near  $T_C$ ,<sup>5</sup> by the MChD effect, and magnetization-induced second harmonic generation (MSHG) effect in GN-(*S*) and GN-(*R*),<sup>9</sup> and also by a theoretical study.<sup>10</sup> In order to investigate the local structure of magnetically ordered phase which might be missed by neutron powder diffraction (NPD) measurements due to a large background from hydrogen atoms,<sup>11</sup> we have performed muon spin rotation and relaxation ( $\mu$ SR) measurements on GN-(*S*) and GN-(*R*).

In this Letter, we show that there are four muon spin precession signals under zero-external field below  $T_C$ , indicating the appearance of a long-range magnetic order and associated multiple muon stopping sites. The internal fields at the muon sites in GN-(*S*) estimated from the muon precession frequencies are consistent with the magnetic dipolar field which is estimated from an average magnetic structure suggested by the NPD measurement. A reasonable set of muon stopping sites are identified near the cyano-bridges without introducing any local modulation of magnetic moments. In addition,  $\mu$ SR measurements in the enantiomer, GN-(*R*), indicates that there is no effective difference in the local magnetic structure from that in GN-(*S*). This is consistent with the presence of a magnetic chirality which, if it exists, should be in conjunction with crystallographic chirality, thereby suggesting that the MChD and MSHG effects in this compound would have closer relevance to the possible absence of inversion symmetry in the magnetic structure.

The GN-(*S*) and GN-(*R*) samples used in this study were obtained by chemical reaction in a solution of  $K_3[Cr(CN_6)]$ ,  $Mn(ClO_4)_2$ , (*S*)-pn-2HCl or (*R*)-pn-2HCl and KOH. For the  $\mu$ SR experiment, a beam of nearly 100% polarized muons with an incident energy of 4 MeV was focused on a target sample. After stopping almost instantaneously at interstitial sites, each muon spin exhibits the Larmor precession under an internal field  $B$  with a frequency  $2\pi f = \gamma_\mu B$  ( $\gamma_\mu = 2\pi \times 135.54$  MHz/T). When the muon decays, an energetic positron is emitted preferentially along the muon spin direction. As a result, the accumulated positron time histograms allow one to monitor the time evolution of muon spin.  $\mu$ SR measurements under zero field (ZF- $\mu$ SR) were conducted at the Muon Science Laboratory, High Energy Accelerator Research Organization (KEK-MSL), Japan and at the Tri-University Meson Facility (TRIUMF), Canada. Powder samples with a net amount of about 0.7 g were mounted on a thick silver sample holder (at KEK-MSL) or on a thin sheet of mylar film (at TRIUMF, where one can obtain background free spectra) and loaded to the  $^4He$  gas flow cryostat. ZF- $\mu$ SR measurements were mainly performed at temperatures between 2 K and room temperature, and additional measurements were performed above  $T_C$  under a transverse field ( $\simeq 2$  mT) to calibrate the instrumental asymmetry and also to check whether or not muonium (a muonic analogue of paramagnetic hydrogen atom) was formed in the samples. The dynamics of local magnetic fields at the muon sites was investigated by  $\mu$ SR measurements under a longitudinal field (LF- $\mu$ SR).<sup>12</sup>

Figure 1 shows the time evolution of the decay positron asymmetry (which is proportional to the time-dependent

muon spin polarization  $P_z(t)$ ) observed in GN-(*R*) under zero field and a longitudinal field at 294 K. The ZF- $\mu$ SR time spectra exhibits exponential damping, indicating that there is a contribution from local electronic moments besides that from randomly oriented nuclear magnetic moments which give rise to a weak Gaussian damping. Therefore, we assume that the time evolution is represented by the sum of diamagnetic and paramagnetic components:

$$A_0 P_z(t, H) = [A_1 + A_2 \exp(-\lambda(H)t)] G_z^{KT}(t, H), \quad (1)$$

$$\lambda(H) \simeq \frac{2\delta_e^2 \nu_e}{\nu_e^2 + \gamma_\mu^2 H^2} \quad (2)$$

where  $A_i$  is the partial asymmetry of each components ( $A_1 + A_2 = A_0$ ),  $G_z^{KT}(t, H)$  is the Kubo-Toyabe relaxation function<sup>13</sup> characterized by the Gaussian damping at early times ( $\sim \exp[-(\Delta t)^2]$ ), followed by the recovery of the polarization to 1/3 when  $H = 0$  (with  $\Delta$  being the rms width of the field distribution arising from the nuclear moments),  $G_z^{KT}(t, H)$  also represents the recovery of polarization with increasing  $H$ ,  $\lambda(H)$  is the relaxation rate due to electronic moments which exert a hyperfine field,  $\delta_e$ , with a fluctuation rate,  $\nu_e$ . Fitting analysis yields  $A_1 = 0.083$  and  $A_2 = 0.147$  (their ratio  $A_1/A_2 \simeq 3/5$ ), and  $\Delta = 0.3(2) \mu s^{-1}$ ,  $\lambda(0) = 0.40(1) \mu s^{-1}$  and  $\lambda(100mT) = 0.14 \mu s^{-1}$ . In order to confirm the presence of two components, we have performed transverse field (TF-)  $\mu$ SR measurements under a field of 1 T. As shown in the inset of Fig. 1, the fast Fourier transform of the TF- $\mu$ SR spectrum has two peaks. The fractional yield of these two peaks is consistent with that of ZF- and LF- $\mu$ SR results,  $A_1$  and  $A_2$ . While it is known that the muon gyromagnetic ratio is often subject to modification by the formation of muonium in insulating compounds, the observed peak frequencies in Fig. 1 inset indicate that no such modification occurs in those samples.

The relaxation rate  $\lambda$  gradually increases with decreasing temperature, which is followed by the appearance of spontaneous muon spin precession signals below 38.5 K in the GN-(*S*) specimen. Figure 2 shows the ZF- $\mu$ SR time spectra near  $T_C$  and those at the lowest temperature. They unambiguously demonstrate that the system falls into the state of a long-range magnetic order below  $T_C$ . Consequently, the data are analyzed by the following function;

$$A_0 P_z(t) = \sum_{i=1}^n A_i^{osc} G_z^{KT}(t) \exp(-\lambda_i^{osc} t) \cos(2\pi f_i t + \phi) + A^{non} G_z^{KT}(t) \exp[-(\lambda^{non} t)^\Gamma] \quad (3)$$

where  $A_i^{osc}$  and  $A^{non}$  are the partial asymmetry of oscillating and non-oscillating components ( $\sum A_i^{osc} + A^{non} = A_0$ ),  $f_i$  is the muon spin precession frequency,  $\lambda_i^{osc}$  and  $\lambda^{non}$  are the relaxation rate, and  $\Gamma$  is the power of the exponent. As mentioned later, we analyzed the data with  $n = 5$  above 30 K, and  $n = 4$  below 30 K.

The temperature dependence of  $f_1$  is shown in Fig. 3. It exhibits a sharp reduction with increasing temperature towards  $T_C$ , where the oscillating component disappears around 39.5 K. These features are common among other

frequency components and consistent with the previous results of magnetization<sup>5</sup> and NPD measurements.<sup>11</sup> The dashed and solid curves in Fig. 3 are fitting results for the data using a form  $(1 - (T/T_C)^\alpha)^\beta$ , where the former is obtained by fixing  $T_C = 38$  K (the value from Ref.<sup>5</sup>), and the latter by letting  $T_C$  vary as a free parameter. The estimated values are  $\alpha = 1.39(16)$ ,  $\beta = 0.38(2)$  and  $T_C = 39.5(1.1)$  K,  $\alpha = 1.41(60)$ ,  $\beta = 0.42(13)$ , respectively. These indices suggest that three-dimensional (3D) interaction is dominant in this system. (e.g.,  $\beta = 0.38$  for 3D Heisenberg magnets) The fast Fourier transform spectrum at 5.5 K is shown in the inset of Fig. 3. As shown in Figs. 2 and 3 inset, the precession signal primarily consists of at least four components (shown by markers in Fig. 3 inset). In particular, it is inferred from the time spectrum at 38.5 K in Fig. 2 that there is an additional high frequency component just below  $T_C$  with a frequency  $f_5 \simeq 92.6(5)$  MHz. Unfortunately, it turns out that this component is not observed below 30 K probably because of the increased frequency that exceeds the current time resolution ( $\sim$  a few ns) at lower temperatures. Note that a peak seen in the inset of Fig. 3 at 3 MHz is not a precession signal but one with a fast relaxation. Their amplitudes at 5.5 K are deduced as  $A_1^{\text{osc}} = 0.011(2)$ ,  $A_2^{\text{osc}} = 0.021(2)$ ,  $A_3^{\text{osc}} = 0.002$ ,  $A_4^{\text{osc}} = 0.004(1)$  and  $A^{\text{non}} = 0.059$ . In the case of polycrystalline samples, it is predicted that  $A^{\text{non}}/A_0$  is close to  $1/3$ , corresponding to the probability that the direction of internal magnetic field is parallel to the initial muon spin direction. However, the observed value of  $A^{\text{non}}/A_0$  is slightly smaller than  $1/3$  (where  $A_0 = 0.23$  at ambient temperature), suggesting a fractional loss of initial polarization due to some unknown process (e.g., muonium formation at low temperatures). More importantly,  $A_0$  is considerably reduced from the value observed at ambient temperature, which is also consistent with the loss of muon polarization at the initial stage of muon implantation. As suggested by the spectrum near  $T_C$ , the missing part of the asymmetry may be attributed to the precession signal(s) which might exhibit unresolved fast precession or relaxation.

We have also performed ZF- and LF- $\mu$ SR measurements in the optical isomer, GN-(*R*). As found in Fig. 2 (b), the ZF- $\mu$ SR spectra observed below  $T_C$  are virtually identical with those in GN-(*S*). A procedure of fitting analysis similar to that for GN-(*S*) has been applied to those data, and components with four different frequencies were identified. The temperature dependence of  $f_1^{\text{GNR}}$  is shown in Fig. 3 (by open triangle), which exhibits perfect agreement with that of GN-(*S*). Thus, the comparison of the results in GN-(*S*) with those in GN-(*R*) indicates that they are magnetically equivalent in the atomic scale.

It is suggested by the results of NPD<sup>11</sup> that the magnetic structure of GN-(*S*) is that of noncollinear ferromagnet with the magnetic (Shubnikov) space group  $P2_12'_12'_1$ , and that the magnetic moments of Cr and Mn atoms are mutually antiparallel along a direction near the *a* axis with their moment size being  $3.84 \mu_B$  and  $5.88 \mu_B$ , respectively. Since the electronic Cr and Mn moments are ordered below  $T_C$ , the observation of multi-

ple components in the precession signals under zero field indicates that there are multiple muon sites. Provided that the local field felt by muon is predominantly due to magnetic dipole field  $\mathbf{H}_{\text{dip}}$ , we have

$$\mathbf{H}_{\text{dip}} = A_{\text{dip}}^{\alpha\beta} \boldsymbol{\mu}_i$$

$$A_{\text{dip}}^{\alpha\beta} = \sum_i \frac{1}{r_i^3} \left( \frac{3\alpha_i\beta_i}{r_i^2} - \delta_{\alpha\beta} \right) \quad (\alpha, \beta = x, y, z), \quad (4)$$

where  $A_{\text{dip}}^{\alpha\beta}$  is the dipole tensor. The sum is over the contribution of the *i*-th  $\text{Cr}^{3+}$  and  $\text{Mn}^{2+}$  ions which have magnetic moments  $\boldsymbol{\mu}_i$  at a distance  $\mathbf{r}_i = (x_i, y_i, z_i)$  from the muon. We can identify the possible muon site by comparing the observed internal field ( $2\pi f_i/\gamma_\mu$ ) and that calculated by the above form with the orientation and moment size of Cr and Mn ions determined by NPD measurements.<sup>11</sup> As noted earlier, we have observed four frequencies below  $T_C$ ,  $f_1 = 45.94(20)$  MHz,  $f_2 = 23.89(13)$  MHz,  $f_3 = 20.39(8)$  MHz and  $f_4 = 17.27(12)$  MHz, yielding the respective local magnetic field at muon sites,  $B_1 = 338.9(1)$  mT,  $B_2 = 176.3(1.0)$  mT,  $B_3 = 150.4(6)$  mT and  $B_4 = 127.4(9)$  mT at the lowest temperature. The comparison strongly suggests that all the muon sites are located near the cyanobridges. This is also supported by the fact that the cyanobase is negatively charged and thereby reduce the electrostatic energy associated with the positive charge of muons. Figure 4 shows the primary candidates for the muon stopping sites for each frequency.

The fact that ZF- $\mu$ SR spectra yields reasonable muon site assignment indicates that the average magnetic structure suggested by NPD (based on the assumption that the muon sites are correctly identified) is close to the actual magnetic structure *without local modulation*. The effectively identical  $\mu$ SR results in GN-(*S*) and GN-(*R*) suggests that the stopping sites of muons are the same in both two samples. As illustrated in Figs. 5a) and 5b), this also suggests that all of the Cr and Mn moments are in the opposite direction with each other between GN-(*R*) and GN-(*S*); otherwise the inversion of crystallographic structure without magnetic structure (as shown in Fig. 5c) would yield different internal fields at the respective muon sites. More specifically, a mirror conversion of  $\mathbf{r}_i$  with reference to *xy*-plane,  $\mathbf{r}_i^* = (x_i, y_i, -z_i)$ , on the dipole tensor leads to the change in the sign of some components (e.g.,  $A_{\text{dip}}^{xx}$ ,  $A_{\text{dip}}^{yy}$ ). As a result, the sum in eq. (4) yields different values between the pair of enantiomers. Thus, we conclude that GN-(*R*) and GN-(*S*) give rise to a complete pair of mirror images in both crystallographic and magnetic structures. Provided that Cr and Mn moments have a small degree of non-collinear character due, for example, to the Dzyaloshinski-Moriya interaction, this immediately leads to a possibility that the system has a chirality in the magnetic structure: the Dzyaloshinski-Moriya interaction is in conjunction with the crystal structure and thus the associated non-collinear spin structure would give rise to the magnetic chirality.<sup>10</sup> Our observation is consistent with the presence of such a chiral magnetic structure conjugating between GN-(*R*) and GN-(*S*).

In summary, we have performed  $\mu$ SR measurements in polycrystalline samples of GN-(*S*) and GN-(*R*) in order to elucidate the local magnetic properties. Muon precession signals were observed under zero field below  $T_C$  in both samples, indicating the presence of long-range ferrimagnetic order which is close to the average magnetic structure suggested by the result of neutron powder diffraction. The identical  $\mu$ SR results obtained in GN-(*S*) and GN-(*R*) indicate that they are a pair of complete optical isomer in terms of both crystallographic and magnetic structure.

We would like to thank the staff of TRIUMF and KEK for their technical support during the experiments. This work was partially supported by a Grant-in-Aid for Creative Scientific Research and a Grant-in-Aid for Scientific Research on Priority Areas by Ministry of Education, Culture, Sports, Science and Technology, Japan.

- 1) G. Wagniere and A. Mejer: Chem. Phys. Lett. **110** (1984) 546.
- 2) G.L.J.A. Rikken and E. Raupach: Nature **390** (1997) 493.
- 3) H. Kumagai and K. Inoue: Angew. Chem. Int. Ed. **38** (1999) 1601.
- 4) K. Inoue, H. Imai, P.S. Ghalsasi, K. Kikuchi, M. Ohba, H. Ōkawa and J.V. Yakhmi: Angew. Chem. Int. Ed. **40** (2001) 4242.
- 5) K. Inoue, K. Kikuchi, M. Ohba and H. Ōkawa: Angew. Chem. Int. Ed. **42** (2003) 4810.
- 6) H. Imai, K. Inoue, K. Kikuchi, Y. Yoshida, M. Ito, T. Sunahara and S. Onaka: Angew. Chem. Int. Ed. **43** (2004) 5618.
- 7) E. Coronado, J.R. Galan-Mascaros, C.J. Gómez-García and J.M. Martínez-Agüero: Inorg. Chem. **40** (2001) 113.
- 8) R. Andréas, M. Bissard, M. Gruselle, C. Train, J. Vaissermann, B. Malézieux, J.-P. Jamet and M. Verdaguer: Inorg. Chem. **40** (2001) 4633.
- 9) K. Inoue *et al.*, to be published.
- 10) J. Kishine, K. Inoue and Y. Yoshida: Prog. Theor. Phys. Suppl. **159** (2005) 82.
- 11) A. Hoshikawa, T. Kamiyama, A. Purwanto, K. Ohishi, W. Higemoto, T. Ishigaki, H. Imai and K. Inoue: J. Phys. Soc. Jpn. **73** (2004) 2597.
- 12) A. Schenck: *Muon Spin Rotation: Principles and Applications in Solid State Physics* (Adam Hilger, Bristol, 1986).
- 13) R. Kubo and T. Toyabe: *Magnetic Resonance and Relaxation* (ed. by R. Blinc, North-Holland, 1967)

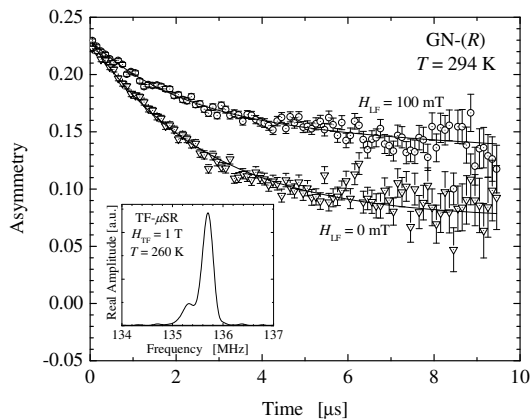


Fig. 1. ZF- and LF- $\mu$ SR time spectra (decay positron asymmetry,  $A_0P_z(t)$ ), in GN-(*R*) at 294 K. The inset shows the fast Fourier transform of the spectrum at 260 K under a transverse field of 1 T (=135.54 MHz).

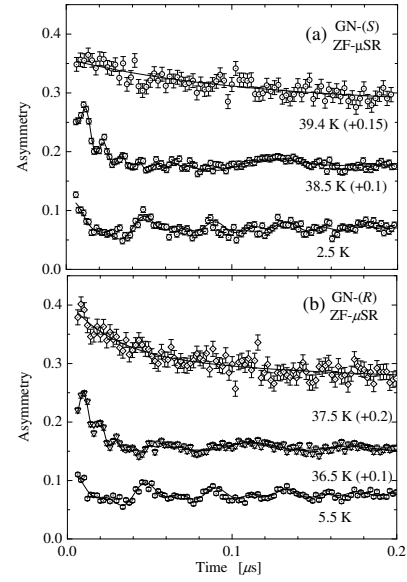


Fig. 2. ZF- $\mu$ SR time spectra ( $A_0P_z(t)$ ) in (a) GN-(*S*) and (b) GN-(*R*) at various temperatures. Note that they are shifted by an equal spacing (0.05 in GN-(*S*) and 0.1 in GN-(*R*)) for clarity, respectively.

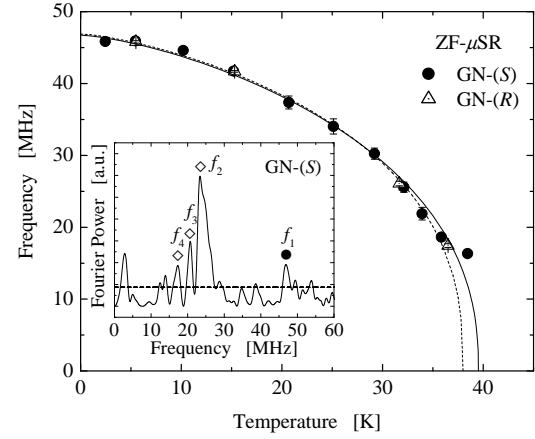


Fig. 3. Temperature dependence of the muon spin precession frequency  $f_1$  in GN-(*S*) and GN-(*R*). Curves show fitting results for the data using a form  $(1 - (T/T_C)^\alpha)^\beta$  with either  $T_C$  fixed to 38 K according to Ref.<sup>5</sup> (dashed), or  $T_C$  varied as a free parameter (solid). The inset shows a fast Fourier transform of the spectrum at 5.5 K. Four frequency peaks are discernible below  $T_C$  which are marked as  $\diamond$  and  $\bullet$ . A peak at  $\sim 3$  MHz is not related to the precession signal.

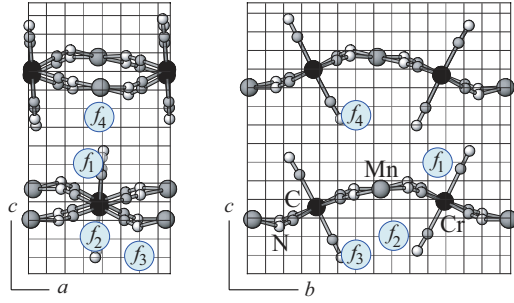


Fig. 4. Muon sites assigned by the comparison between the observed internal fields and calculated dipolar fields based on a magnetic structure suggested by NPD. Crystal structure of GN(*S*) are displayed only for Cr, Mn and cyano-bridges in the unit cell. Sublattice stands for a 1Å space.

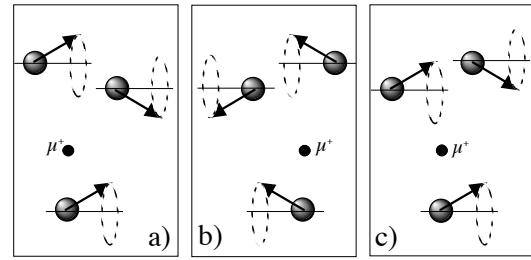


Fig. 5. a) A schematic illustration of atomic configurations in a unit cell with crystallographic and magnetic chirality (where the arrows indicate magnetic moments). A complete mirror inversion of (a) in terms of both atomic and magnetic configuration is shown in (b), whereas (c) corresponds to that only for the crystallographic part. The internal field at a muon site (labeled  $\mu^+$ ) is common between (a) and (b) but it would be different with (c) when the magnetic moments are non-collinear.